Modulation-induced frequency shifts in a coherent-population-trapping-based atomic clock

David F. Phillips, Irina Novikova, Christine Y.-T. Wang, and Ronald L. Walsworth

Harvard–Smithsonian Center for Astrophysics, Cambridge, Massachusetts 02138

Michael Crescimanno

Department of Physics and Astronomy, Youngstown State University, Youngstown, Ohio 44555

Received April 12, 2004; revised manuscript received August 2, 2004; accepted August 26, 2004

We investigate systematic errors associated with a common modulation technique used for phase-sensitive detection of a coherent-population-trapping (CPT) resonance. In particular, we show that modification of the CPT resonance line shape due to the presence of off-resonant fields leads to frequency shifts that may limit the stability of CPT-based atomic clocks. We also demonstrate that an alternative demodulation technique greatly reduces these effects. © 2005 Optical Society of America

OCIS codes: 020.1670, 020.3690, 120.3930, 300.6380.

Coherent population trapping[1] (CPT) has recently been applied to the development of small stable clocks with observed fractional frequency stability (Allan deviation) of better than $10^{-11}\,\tau^{-1/2}$ for averaging times, τ, around 100 s.[2–5] CPT clocks have potential advantages relative to traditional intensity optical pumping clocks (which typically employ an optical and microwave double-resonance technique)[2] including the possibility of substantial miniaturization without degradation of performance.[6,7] However, various mechanisms may degrade the frequency stability of CPT clocks below that theoretically expected from the observed signal-to-noise ratio. One key mechanism for such degradation is conversion of FM laser noise to AM noise in the detected CPT transmission signal, owing to the optical absorption profile when a laser with a large linewidth is used.[8,9] Here we demonstrate a second important degradation mechanism: a widely used, slow-phase-modulation technique leads to shifts of the clock frequency in the presence of asymmetries in the CPT resonance. We also show that a straightforward variation of this modulation technique (i.e., use of third-harmonic demodulation) can eliminate much of the systematic effect on the clock frequency.

A CPT clock employs two optical fields that are nominally resonant with electronic transitions in alkali atoms such as Rb or Cs, with the frequency difference between the optical fields being equal to the hyperfine splitting of the alkali's electronic ground state. Initially, these two fields optically pump the atoms into a noninteracting coherent superposition of two hyperfine states (a dark state).[1] The long relaxation time of the electronic ground state leads to enhanced transmission of the optical fields in a narrow resonance around the difference frequency of the two optical fields. The center frequency of this resonance serves as the CPT clock frequency; the width of the resonance is determined by the decoherence rate of the dark state.

In the typical manifestation of a CPT clock, a current-modulated diode laser produces the two resonant optical fields (Fig. 1). Such a laser, with an optical frequency ν_{opt} and modulated at a microwave frequency ν_μ, generates an electric field

$$\begin{aligned}\varepsilon = {} & \varepsilon_0 \cos 2\pi\nu_{\mathrm{opt}} t \\ & + \varepsilon_{-1} \cos 2\pi(\nu_{\mathrm{opt}} - \nu_\mu)t + \varepsilon_{+1} \cos 2\pi(\nu_{\mathrm{opt}} + \nu_\mu)t \\ & + \varepsilon_{-2} \cos 2\pi(\nu_{\mathrm{opt}} - 2\nu_\mu)t + \varepsilon_{+2} \cos 2\pi \\ & \times (\nu_{\mathrm{opt}} + 2\nu_\mu)t + \ldots, \end{aligned} \tag{1}$$

where ε_i are the amplitudes of the various frequency components of the electric field. The corresponding Rabi frequencies for the atomic transitions driven by the fields are $\Omega_i = d_i\varepsilon_i/(2\hbar)$, where d_i is the atomic transition dipole moment. If the modulation frequency is equal to half the ground-state hyperfine splitting ($\nu_\mu = \Delta_{\mathrm{hfs}}/2$) and the laser carrier (ν_{opt}) is tuned midway between the electronic transition frequencies for the ground-state hyperfine sublevels, then the first-order (± 1) sidebands are simultaneously resonant with the electronic transitions for the two hyperfine sublevels, and a maximum optical transmission is observed. However, additional off-resonant fields are also created by the laser current modulation. (The carrier, Ω_0, and the second-order sidebands, $\Omega_{\pm 2}$, are generally the most significant off-resonant fields.) Even though these fields are far detuned from the atomic resonances, they induce an ac Stark shift, which depends on both the optical field frequency and the intensity and causes a relative shift in the atomic levels (a light shift in the CPT clock frequency). This sensitivity of the CPT resonance to laser detuning and intensity can limit the stability of a CPT clock. Fortunately, with careful choice of a current-modulation index, ac Stark shifts from different off-resonant fields can be arranged to cancel one another.[2]

Phase-sensitive detection is often used to provide a sensitive feedback signal for the local oscillator (e.g., a quartz

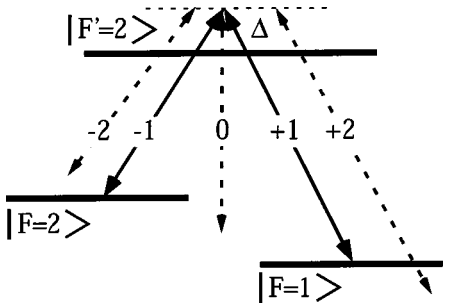

Fig. 1. Energy-level diagram for a three-level atom coupled via two near-resonant fields: the +1 and −1 sidebands from a modulated carrier laser field, with one-photon detuning Δ. Also shown are nonresonant fields (the carrier, 0, and the +2 and −2 sidebands), which can produce shifts and distortions in the CPT resonance. For the current experiments that use ^{87}Rb, the two lower levels correspond to the ground-electronic-state hyperfine levels $F = 2$ and $F = 1$; the upper level corresponds to $5^2P_{1/2}F' = 2$.

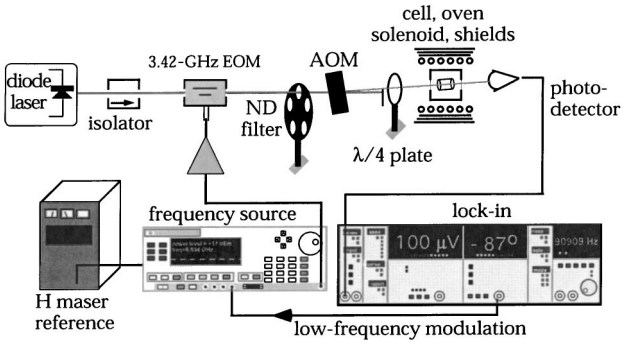

Fig. 2. Schematic of the apparatus.

crystal) that is typically locked to the CPT resonance to make a functioning clock. Typically, a slow (<1-kHz) phase modulation is superimposed on the microwave source, leading to a modification of the phase of the microwave drive:

$$2\pi\nu_\mu t \rightarrow 2\pi\nu_\mu t + \epsilon \sin(2\pi f_m t), \tag{2}$$

where f_m is the modulation frequency and ϵ is the modulation index. After demodulation, the (approximately) symmetric CPT transmission resonance is transformed into an (approximately) antisymmetric dispersionlike signal. Near an exactly symmetric CPT resonance, this dispersionlike signal is proportional to the frequency difference between the local oscillator and the center of the CPT resonance, and thus one can lock the local oscillator exactly to the CPT resonance by measuring the microwave frequency (ν_μ) corresponding to the zero crossing of the dispersionlike signal. However, any asymmetry in the CPT transmission resonance line shape shifts the zero crossing of the dispersionlike signal, with a magnitude dependent on the slow-phase-modulation parameters. Instability in these modulation parameters will thus induce instability in the CPT clock's microwave frequency. Here we present a detailed experimental study of such shifts and demonstrate that the main contribution is made by the far-detuned optical carrier, Ω_0 (designated as field "0" in Fig. 1). Note that, in principle, the slow phase modulation and the resultant systematic effects on CPT clock performance may be eliminated. For example, the microwave signal that modulates the laser may be produced by direct feedback from a fast output photodetector.[10]

Figure 2 shows a schematic of our experimental setup. We derived the two optical fields needed for the CPT clock by phase modulating the output from an external-cavity diode laser[11] tuned in the vicinity of the D_1 line of Rb ($5^2S_{1/2} \rightarrow 5^2P_{1/2}$, $\lambda \simeq 795\,\mathrm{nm}$). An electro-optic modulator (EOM)[12] produced the phase modulation of the optical field at half of the ground-state hyperfine frequency of ^{87}Rb ($\Delta_{\mathrm{hfs}} \simeq 6.8\,\mathrm{GHz}$). With the microwave power available to the EOM in these measurements (roughly 1 W), approximately 15% of the incident laser power was transferred to all sidebands, with the remainder residing in the off-resonant carrier. Ideally, the EOM should produce equal amplitudes in the ±1 sidebands, but, owing to a slight misalignment of the input polarization, the +1 sideband was 1.3 dB larger than the −1 sideband, producing a 35% larger Rabi frequency (Ω_{+1}) for the $|F = 1\rangle \rightarrow |F' = 2\rangle$ transition than the Rabi frequency (Ω_{-1})$|F = 2\rangle \rightarrow |F' = 2\rangle$ transition. Following the EOM, all the optical fields were attenuated by a neutral-density (ND) filter and an acousto-optic modulator (AOM) to approximately 10-μW total power, circularly polarized with a quarter-wave (λ/4) plate, and then weakly focused to a diameter of approximately 0.8 mm as they passed through a Rb vapor cell.

The vapor cell was placed inside three layers of high-permeability magnetic shielding to screen out external fields, with a solenoid also inside the magnetic shields to control the magnetic field. The 2.5-cm-diameter, 5-cm-long vapor cell contained a natural abundance of Rb and 5 Torr of nitrogen buffer gas. The buffer gas slowed the Rb atomic motion through the vapor cell. The vapor cell was thermally stabilized by use of a blown-air oven at a temperature of 45 °C. The total Rb vapor pressure at this temperature corresponds to a ^{87}Rb atomic density of $2 \times 10^{10}\,\mathrm{cm}^{-3}$. Under these conditions the optical depth of the vapor cell was approximately 1, for a weak resonant optical field.

A coupled, three-level Λ system was formed by the two first-order sidebands of the laser field; the two lower ^{87}Rb states $F = 1$, $m_F = 0$ and $F = 2$, $m_F = 0$; and the excited state $F' = 2$, $m_{F'} = 1$ (Fig. 1). We chose these hyperfine sublevels so as to have no first-order dependence of hyperfine transition frequency on the magnetic field. We applied a magnetic field of 16 mG to lift Zeeman degeneracies and remove other ground-state sublevels from two-photon resonance, thus preventing unwanted coherences from developing.

We used phase-sensitive detection to convert the approximately symmetric CPT transmission resonance of the two-photon clock transition into a dispersivelike resonance (Fig. 3). We applied a slow phase modulation to the microwave source driving the EOM and then demodulated the corresponding slow variations in the photodetector current by using a lock-in amplifier. In a working CPT clock, a feedback loop locks the external oscillator to the zero crossing of the antisymmetric, modulated line. Here, rather than closing the loop in the feedback system, we measured the frequency of the zero crossing (by fitting a line through the central part of the dispersivelike reso-

nance) relative to a frequency source phase locked to a H maser. We then varied system parameters such as the laser detuning (ν_{opt}), slow-phase-modulation frequency (f_m), or modulation index (ϵ) and measured the zero crossing as a function of these parameters.

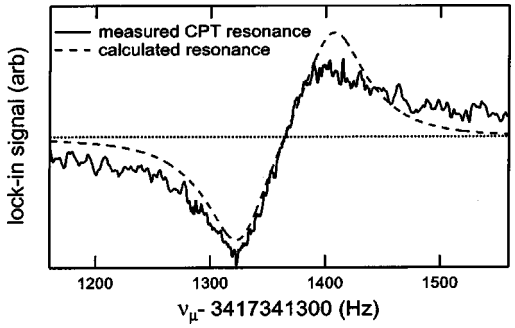

Fig. 3. Typical dispersivelike CPT resonance measured with a slow-phase-modulation frequency $f_m = 230$ Hz and index $\epsilon = 0.6$ (solid curve). Also shown is a numerical calculation of the line shape expected from an ideal three-level system and just two near-resonant optical fields, for our observed Rabi frequencies and slow-phase-modulation index (dotted line). (The width and center frequency of the calculated resonance were scaled to match the measured resonance.) Note the asymmetry of the measured resonance compared with the calculation for the ideal three-level, two-field system.

Drifts in the zero crossing will directly lead to changes in the clock frequency and thus degrade the frequency stability of the CPT clock. To characterize such variations in the clock frequency (δ), we measured the dependence of the zero crossing on the laser carrier detuning (Δ), for various slow-phase-modulation (i.e., lock-in) parameters. (Note that Δ was also the detuning of the first-order sidebands from the center of the Doppler-broadened absorption resonance.) Figure 4(a) shows the measured clock frequency shift as a function of laser detuning for various slow-phase-modulation (lock-in) indices at one fixed laser modulation index (EOM power). We find that, near the center of the Doppler-broadened atomic transition, the clock frequency is proportional to the laser detuning [see the linear fits in Fig. 4(a)], with a slope δ/Δ that increases linearly with slow-phase-modulation index (at fixed slow-phase-modulation frequency) as shown on Fig. 4(b). We observed similar behavior on changing the slow-phase-modulation frequency at fixed slow phase-modulation index. These shifts are significant in comparison with the desired frequency stability of a CPT clock, with fractional clock frequency sensitivity to laser detuning of order 10^{-11}/MHz. As shown in Fig. 4(c), we

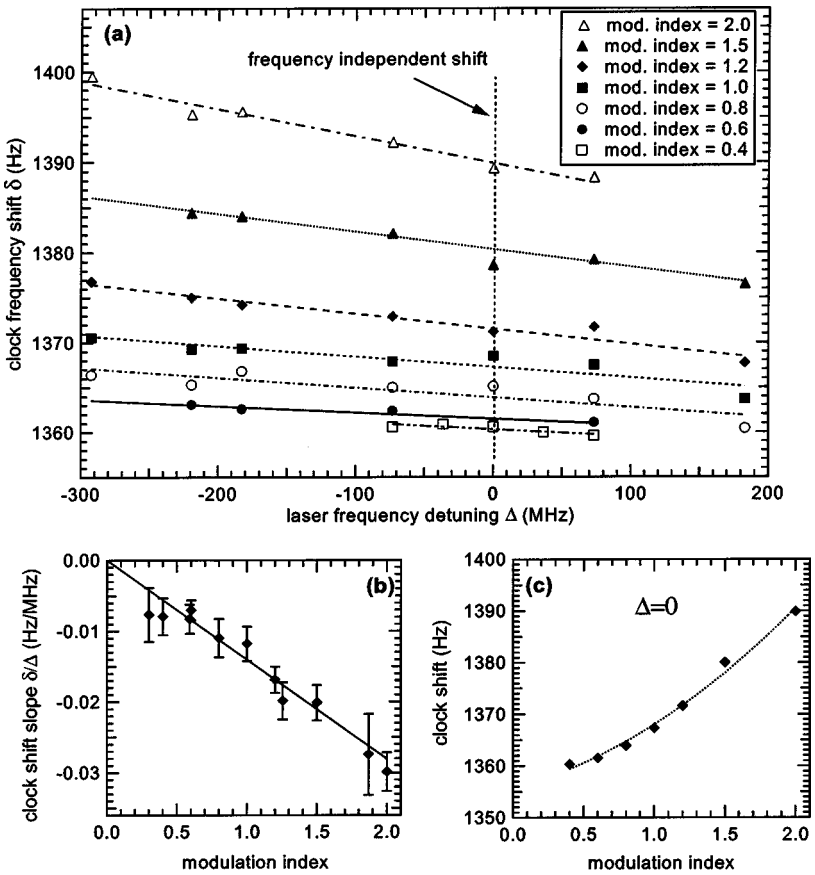

Fig. 4. (a) Measured ^{87}Rb CPT clock frequency shift (δ) as a function of detuning (Δ) of the laser carrier frequency and resonant sidebands from $F' = 2$ resonance, for various slow-phase-modulation indices (ϵ). Here a zero frequency shift ($\delta = 0$) corresponds to the free-space ^{87}Rb hyperfine frequency. The large offset of $\delta \approx 1360$ Hz is due to the nitrogen buffer-gas pressure shift. (b) Dependence of the clock frequency on laser detuning (δ/Δ), determined from the slope of each individual line on plot (a), as a function of the slow-phase-modulation index. (c) Measured laser-frequency-independent shift, at $\Delta = 0$, as a function of the slow-phase-modulation index [see vertical line in plot (a)]. All data were taken at a slow-phase-modulation (lock-in) frequency $f_m = 69$ Hz. In graphs (a) and (c), measurement uncertainties were comparable with the size of the symbols shown.

also observed a dependence of the clock frequency on the slow-phase-modulation index, with the laser fields tuned to resonance, i.e., with $\Delta = 0$. This laser-frequency-independent shift is of order 10^{-8} (fractionally) for 100% changes in the modulation index. Good CPT clock frequency stability therefore requires high stability of the slow-phase-modulation frequency and amplitude, even in the absence of laser frequency variation.

Light shifts (i.e., ac Stark shifts) associated with unequal intensities of the first-order laser sidebands[13,14] are expected to scale linearly with the laser detuning:

$$\delta \propto -\Delta \frac{|\Omega_{+1}|^2 - |\Omega_{-1}|^2}{\gamma^2}, \tag{3}$$

where $\Omega_{\pm 1}$ are the Rabi frequencies of the resonant laser sidebands and γ is the relaxation rate of the excited state. The data in Fig. 4(a) exhibit this linear scaling of δ with Δ. However, this simple light-shift mechanism does not account for the observed dependence of the clock frequency on the slow-phase-modulation index [see Figs. 4(b) and 4(c)]. The above light-shift expression assumes that the CPT resonance remains symmetric near the center, shifting only because of the Rabi frequency difference. However, as shown in Fig. 4, the clock frequency shift (δ) depends on the modulation index (ϵ), indicating that the CPT resonance is asymmetric. [A similar dependence of δ on the slow-phase-modulation frequency (f_m) was also observed (Fig. 7a).] Additionally, these dependencies do not vanish at $\Delta = 0$, indicating that other frequency-shift mechanisms are present.

One such mechanism is the light shift caused by the off-resonant carrier field. As with the Rabi frequency imbalance described above, this light shift is usually expected to cause a simple shift in the clock frequency but no distortion of the line shape. The shift is expected to be $\simeq 2|\Omega_0|^2/\Delta_0$, where Ω_0 is the carrier field Rabi frequency and $\Delta_0 = \Delta_{\mathrm{hfs}}/2$ is the magnitude of the carrier's detuning from both transitions in the Λ system for $\Delta = 0$. Without a distortion of the line shape, no dependence of the clock frequency shift (δ) on the slow-phase-modulation parameters should exist. Figure 5 shows the measured clock frequency shift as a function of laser carrier field power ($\sim|\Omega_0|^2$) at two slow-phase-modulation frequencies and two total powers in the first-order sidebands, all for $\Delta = 0$. In addition to the usual light shift, we observe a dependence on the slow-phase-modulation frequency of approximately (20 mHz/μW)/Hz. Consistent with expression (3) at $\Delta = 0$, we do not find a dependence of δ on the first-order sideband power, $|\Omega_{\pm 1}|$. From these measurements, we conclude that the interaction of the strong, off-resonant carrier field of the modulated laser not only shifts the clock frequency but also modifies the transmission resonance line shape.

To further study the dependence of the clock frequency on the carrier field, we inserted a Fabry–Perot cavity between the EOM and the vapor cell in a slightly altered experimental setup.[15] This cavity had a free spectral range of 1.37 GHz (one fifth of the ^{87}Rb hyperfine splitting) and was tuned such that it allowed the transmission of the two first-order sidebands of the laser while rejecting the carrier frequency field. A more symmetric output signal

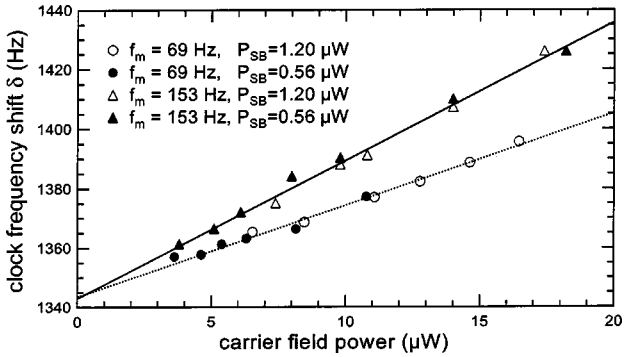

Fig. 5. Measured dependence of the CPT clock frequency on carrier field power at one-photon resonance ($\Delta = 0$), for two slow-phase-modulation frequencies and two total powers in the first-order sidebands. (Uncertainties in the measured clock frequencies are approximately equal to the size of the points.) Linear fits are shown for all data points at each of the two modulation frequencies.

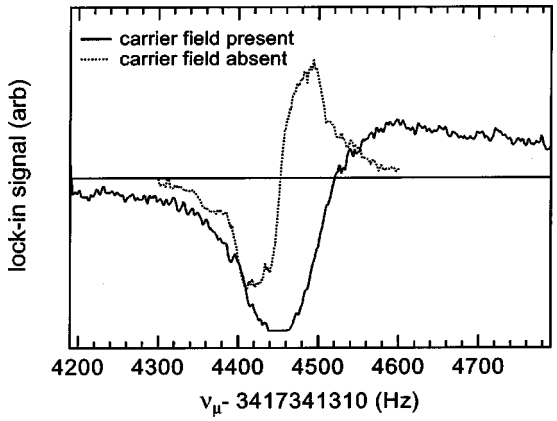

Fig. 6. CPT resonances with (solid curve) and without (dotted curve) the carrier field present. Both data sets were taken with $f_m = 98$ Hz and $\epsilon \approx 0.6$ and with a vapor cell containing isotopically enriched ^{87}Rb and 22 Torr of Ne buffer gas.[15]

was detected (see Fig. 6), and the dependence of the clock frequency shifts on the slow-phase-modulation parameters (ϵ and f_m) was reduced by at least an order of magnitude.

We explored alternative techniques for slow phase modulation with the goal of reducing the dependence of the CPT clock frequency on system parameters. For example, we investigated demodulation by using the third harmonic of the slow phase modulation, a technique that is known to compensate for linear asymmetry in an underlying resonance.[16,17] We found that the clock frequency for both first- and third-harmonic demodulations has a linear dependence on the slow modulation frequency [Fig. 7(a)]. However, with third-harmonic demodulation, the slope of this dependence is a factor of 5 smaller, reducing the sensitivity of the clock frequency to changes in either the laser carrier frequency [e.g., Fig. 4(a)] or the properties of the slow-phase-modulation source [Figs. 4(a) and 4(b)]. Similarly, we found that third-harmonic demodulation reduces the laser-frequency-independent shift by at least an order of magnitude to fractional shifts of less than 10^{-9} for 100% changes in modulation index.

One must also consider the change in measurement sensitivity to the clock transition when changing the slow-phase-modulation technique. We define the measurement sensitivity as the ratio of the fitted central slope of the dispersivelike resonance divided by the rms fluctuations in the fit residuals. Optimal measurement sensitivity occurs for the slow-phase-modulation index and frequency that provide maximum signal at the photodetector in the slow-phase-modulation sidebands demodulated by the lock-in amplifier. This optimal sensitivity is achieved when the width of the comb of slow-phase-modulation sidebands transmitted through the atomic medium is comparable with the CPT resonance width. At the optimal slow-phase-modulation index for first-harmonic demodulation, we found that the measurement sensitivity when third-harmonic demodulation was used is substantially reduced; however, we recovered the original sensitivity by increasing the slow-phase-modulation index [Fig. 7(b)].

The measurement sensitivity's dependence on modulation index is consistent with a simple Lorentzian model. We calculated the dispersive curves obtained by applying slow modulation at frequency f_m and index ϵ to a Lorentzian line shape and determined the slope of the curve near the zero crossing. The curves in Fig. 7(b) show this slope as a function of modulation index with only the ratio of the Lorentzian resonance linewidth to the modulation frequency and the overall amplitude adjusted to fit the data. Note, however, that this model does not include a realistic CPT line shape or the effects of off-resonant fields and thus does not reproduce the data in Fig. 7(a).

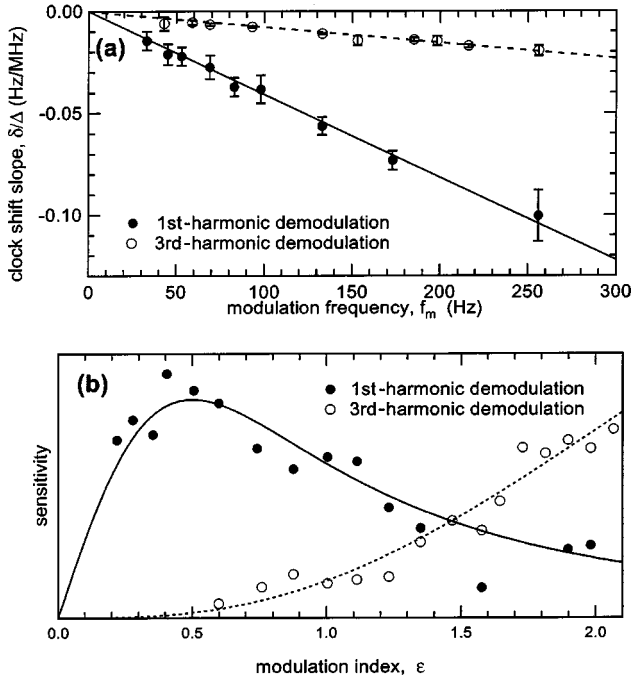

Fig. 7. (a) Clock frequency dependence on laser frequency (δ/Δ) as a function of slow-phase-modulation frequency (f_m) for both first- and third-harmonic demodulations. The modulation index $\epsilon = 1.87$ for both data sets. (b) Dependence of the clock transition's measurement sensitivity (defined in text) on the slow-phase-modulation index (ϵ) for $f_m = 153$ Hz. A much larger slow-phase-modulation index is required for optimal sensitivity in third-harmonic modulation. The lines are the results of a fit to the sensitivity expected for an ideal Lorentzian line shape.

In conclusion, we have quantitatively studied systematic effects on CPT clock frequency due to asymmetries in the two-photon CPT resonance induced by strong off-resonant laser fields. These asymmetries can produce significant shifts in the CPT clock frequency when slow phase modulation is used to determine the center of the CPT resonance. While lowering the frequency of the slow phase modulation decreases the sensitivity of the clock to such systematic frequency shifts, technical noise reduces the signal-to-noise ratio (and hence the clock's short-term frequency stability) at slow-phase-modulation frequencies.

To achieve good fractional frequency stability of $\sim 10^{-11}$ in a CPT clock, these systematic frequency shifts impose demanding requirements on the stability of the elements that control the slow phase modulation (f_m and ϵ) and the laser carrier frequency (ν_{opt}). Fortunately, there are promising alternative modulation techniques that can mitigate the effects of CPT line-shape asymmetry in the presence of nonresonant laser fields. A careful choice of the fast (microwave) modulation index allows the ac Stark shifts from different off-resonant laser fields to cancel each other.[2] As demonstrated here, third-harmonic demodulation of the slow phase modulation greatly reduces the sensitivity to asymmetry in the CPT resonance.

ACKNOWLEDGMENTS

We thank R. F. C. Vessot and E. M. Mattison for technical assistance. B. Murphy and J. Hager contributed to early aspects of this paper. This research was supported by the Office of Naval Research and in part by the National Science Foundation through a grant to the Institute of Theoretical Atomic and Molecular Physics at Harvard University and the Smithsonian Astrophysical Observatory.

D. F. Phillips, the corresponding author, may be reached by e-mail at dphil@cfa.harvard.edu.

REFERENCES AND NOTES

1. E. Arimondo, "Coherent population trapping in laser spectroscopy," Prog. Opt. **35**, 257–354 (1996).
2. J. Vanier, M. W. Levine, D. Janssen, and M. J. Delaney, "On the use of intensity optical pumping and coherent population trapping techniques in the implementation of atomic frequency standards," IEEE Trans. Instrum. Meas. **52**, 822–831 (2003).
3. J. Kitching, S. Knappe, N. Vukičevič, L. Hollberg, R. Wynands, and W. Weidmann, "A microwave frequency reference based on VCSEL-driven dark line resonances in Cs vapor," IEEE Trans. Instrum. Meas. **49**, 1313–1317 (2000).
4. S. Knappe, R. Wynands, J. Kitching, H. G. Robinson, and L. Hollberg, "Characterization of coherent population-trapping resonances as atomic frequency references," J. Opt. Soc. Am. B **18**, 1545–1553 (2001).
5. M. Merimaa, T. Lindvall, I. Tittonen, and E. Ikonen, "All-optical atomic clock based on coherent population trapping in ^{85}Rb," J. Opt. Soc. Am. B **20**, 273–279 (2003).
6. J. Kitching, S. Knappe, and L. Hollberg, "Miniature vapor-cell atomic-frequency references," Appl. Phys. Lett. **81**, 553–555 (2002).

7. S. Knappe, L. Hollberg, and J. Kitching, "Dark-line atomic resonances in submillimeter structures," Opt. Lett. **29**, 388–390 (2004).
8. J. Kitching, H. G. Robinson, L. Hollberg, S. Knappe, and R. Wynands, "Optical-pumping noise in laser-pumped, all-optical microwave frequency references," J. Opt. Soc. Am. B **18**, 1676–1682 (2001).
9. J. C. Camparo and W. F. Buell, "Laser PM to AM conversion in atomic vapors and short term clock stability," in *Proceedings of the 1997 IEEE International Frequency Control Symposium* (IEEE, Piscataway, N.J., 1997), pp. 253–258 (1997).
10. D. Strekalov, D. Aveline, N. Yu, R. Thompson, A. B. Matsko, and L. Maleki, "Stabilizing an optoelectronic microwave oscillator with photonic filters," J. Lightwave Technol. **21**, 3052–3061 (2003).
11. New Focus Vortex laser, Model 6017.
12. New Focus phase modulator, Model 4431.
13. S. Knappe, M. Stähler, C. Affolderbach, A. V. Taĭchenachev, V. I. Yudin, and R. Wynands, "Simple parametrization of dark-resonance line shapes," Appl. Phys. B **76**, 57–63 (2003).
14. A. V. Taĭchenachev, V. I. Yudin, R. Wynands, M. Stähler, J. Kitching, and L. Hollberg, "Theory of dark resonances for alkali-metal vapors in a buffer-gas cell," Phys. Rev. A **67**, 033810 (2003).
15. For this series of measurements, we used a vapor cell with isotopically enriched ^{87}Rb and 22 Torr of Ne buffer gas. The change in buffer gas leads to both a different overall clock frequency shift and a narrower CPT resonance than the 5 Torr N_2 cell we used for the other measurements we report here.
16. F. L. Walls, "Errors in determining the center of a resonance line using sinusoidal frequency (phase) modulation," IEEE Trans. Ultrason. Ferroelectr. Freq. Control **34**, 592–597 (1987).
17. A. de Marchi, G. D. Rovera, and A. Premoli, "Effects of servo loop modulation in atomic beam frequency standards employing a Ramsey cavity," IEEE Trans. Ultrason. Ferroelectr. Freq. Control **34**, 582–591 (1987).